

# Supplementary Material

**Zheyi Dong**<sup>1,2,3,4,5,+</sup>, **Xiaofei Wang**<sup>6,7,+</sup>, **Sai Pan**<sup>1,2,3,4,5,+</sup>, **Taohan Weng**<sup>7,+</sup>, **Xiaoniao Chen**<sup>8,9,+</sup>, **Shuangshuang Jiang**<sup>1,2,3,4,5,10</sup>, **Ying Li**<sup>11</sup>, **Zonghua Wang**<sup>12</sup>, **Xueying Cao**<sup>1,2,3,4,5</sup>, **Qian Wang**<sup>1,2,3,4,5</sup>, **Pu Chen**<sup>1,2,3,4,5</sup>, **Lai Jiang**<sup>7</sup>, **Guangyan Cai**<sup>1,2,3,4,5</sup>, **Li Zhang**<sup>1,2,3,4,5</sup>, **Yong Wang**<sup>1,2,3,4,5</sup>, **Jinkui Yang**<sup>13</sup>, **Yani He**<sup>14</sup>, **Hongli Lin**<sup>15</sup>, **Jie Wu**<sup>1,2,3,4,5</sup>, **Li Tang**<sup>1,2,3,4,5</sup>, **Jianhui Zhou**<sup>1,2,3,4,5</sup>, **Shengxi Li**<sup>7</sup>, **Zhaohui Li**<sup>10</sup>, **Yibing Fu**<sup>7</sup>, **Xinyue Yu**<sup>10</sup>, **Yanqiu Geng**<sup>16</sup>, **Yingjie Zhang**<sup>1,2,3,4,5</sup>, **Liqiang Wang**<sup>8,\*</sup>, **Mai Xu**<sup>7,\*</sup>, and **Xiangmei Chen**<sup>1,2,3,4,5,\*</sup>

<sup>1</sup>Department of Nephrology, First Medical Center of Chinese People's Liberation Army General Hospital, Beijing, China.

<sup>2</sup>Nephrology Institute of the Chinese People's Liberation Army, Beijing, China.

<sup>3</sup>State Key Laboratory of Kidney Diseases, Beijing, China.

<sup>4</sup>National Clinical Research Center for Kidney Diseases, Beijing, China.

<sup>5</sup>Beijing Key Laboratory of Kidney Disease Research, Beijing, China.

<sup>6</sup>Department of Clinical Neurosciences, University of Cambridge, UK.

<sup>7</sup>School of Electronic and Information Engineering, Beihang University, Beijing, China.

<sup>8</sup>Senior Department of Ophthalmology, Third Medical Center of Chinese PLA General Hospital, Beijing, China.

<sup>9</sup>Beijing Tongren Eye Center, Beijing Tongren Hospital, Capital Medical University, Beijing, China.

<sup>10</sup>School of Clinical Medicine, Guangdong Pharmaceutical University, Guangzhou, China.

<sup>11</sup>Department of Ophthalmology, First Medical Center of Chinese PLA General Hospital, Beijing, China.

<sup>12</sup>Department of Ophthalmology, Seventh Medical Center of Chinese PLA General Hospital, Beijing, China.

<sup>13</sup>Beijing Key Laboratory of Diabetes Research and Care, Beijing Diabetes Institute, Beijing Tongren Hospital, Capital Medical University, Beijing, China.

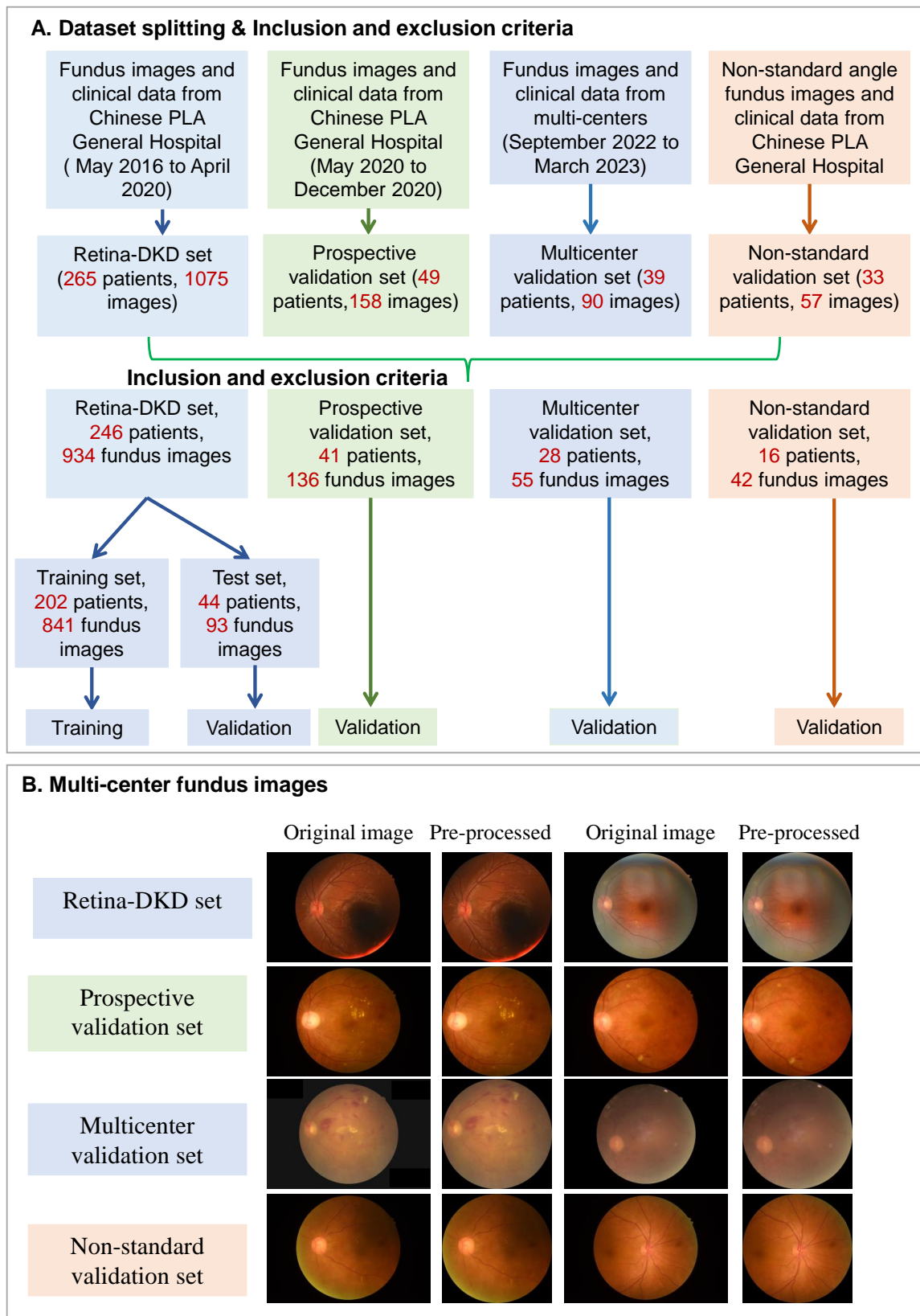
<sup>14</sup>Department of nephrology, Daping Hospital, Army Medical University, Chongqing, China.

<sup>15</sup>The First Affiliated Hospital of Dalian Medical University Key Laboratory of Kidney Disease, Center for the Transformation Medicine of Kidney Disease, Dalian, China.

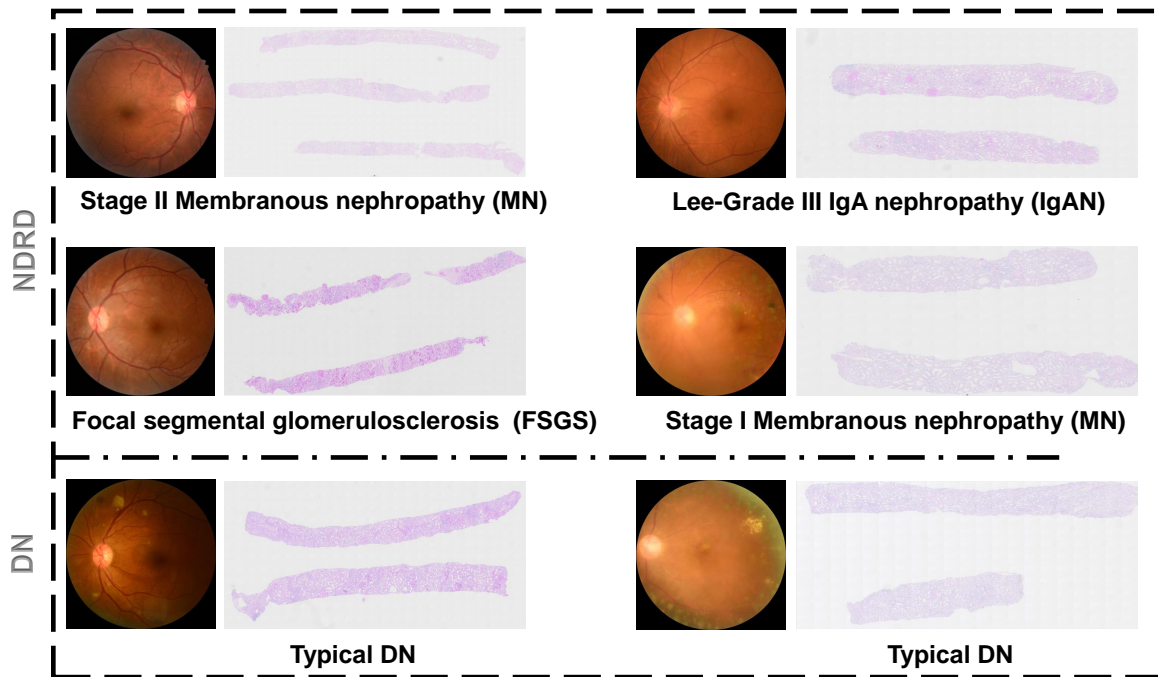
<sup>16</sup>Department of Nephrology, Third Medical Center of Chinese PLA General Hospital, Beijing, China.

\*Xiangmei Chen, Mai Xu and Liqiang Wang are co-corresponding authors (xmchen301@126.com; MaiXu@buaa.edu.cn; liqiangw301@163.com)

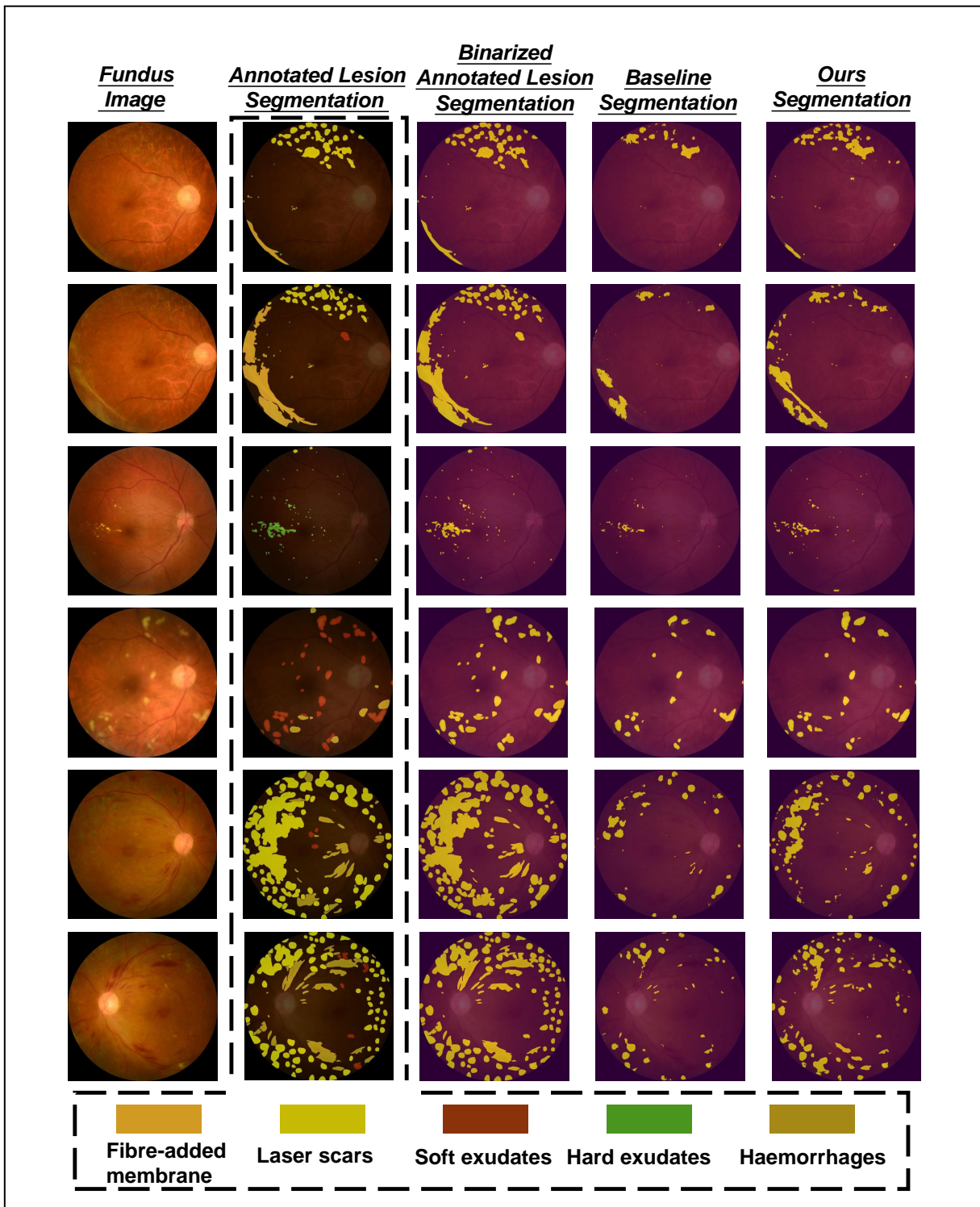
+Zheyi Dong, Xiaofei Wang, Sai Pan, Taohan Weng, and Xiaoniao Chen contribute equally to this work.



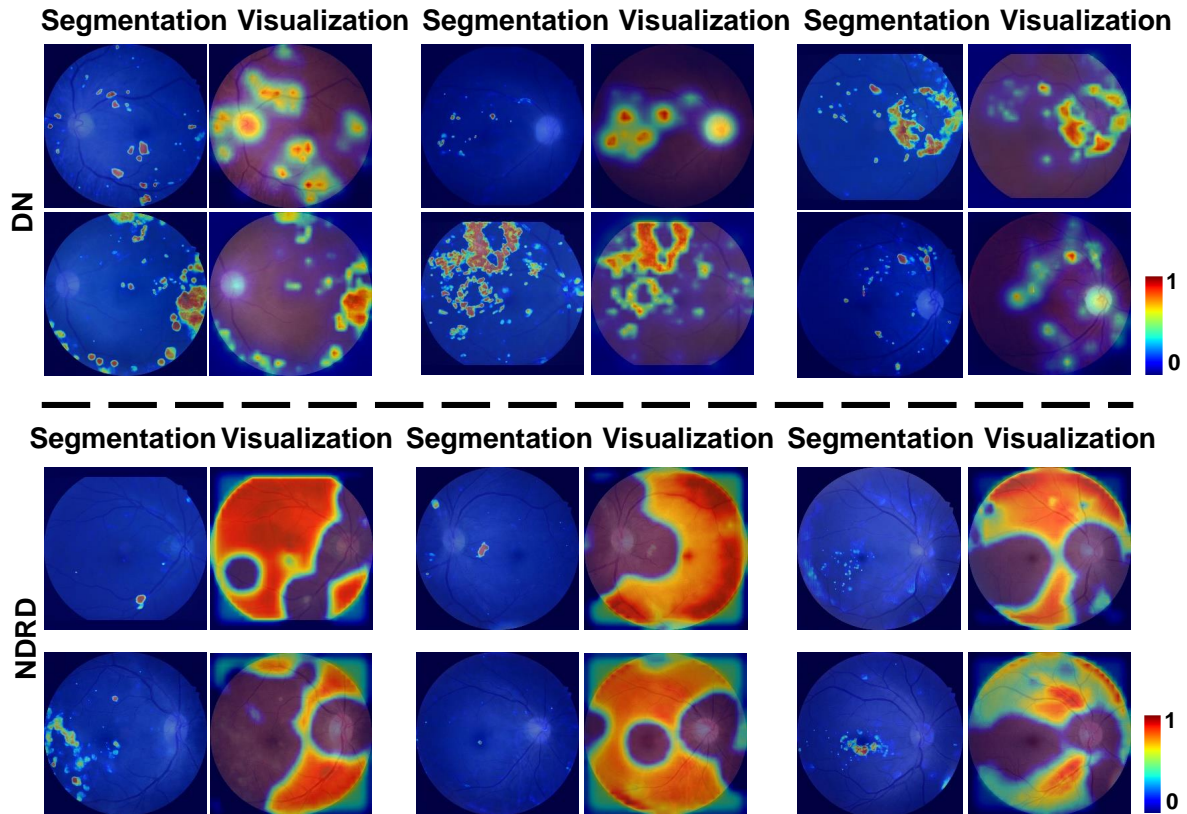
**Supplementary Figure 1. Data collection and fundus image presentation.** (A) Illustration of dataset splitting as well as patient inclusion and exclusion criteria (B) Illustration of the original and pre-processed retinal fundus images of the four involved datasets.



**Supplementary Figure 2. Fundus images and pathological images of the same patient.** Illustration of the hematoxylin and eosin (H&E) stained histopathological images and correlated fundus images of DN and NDRD in the Retina-DKD set.



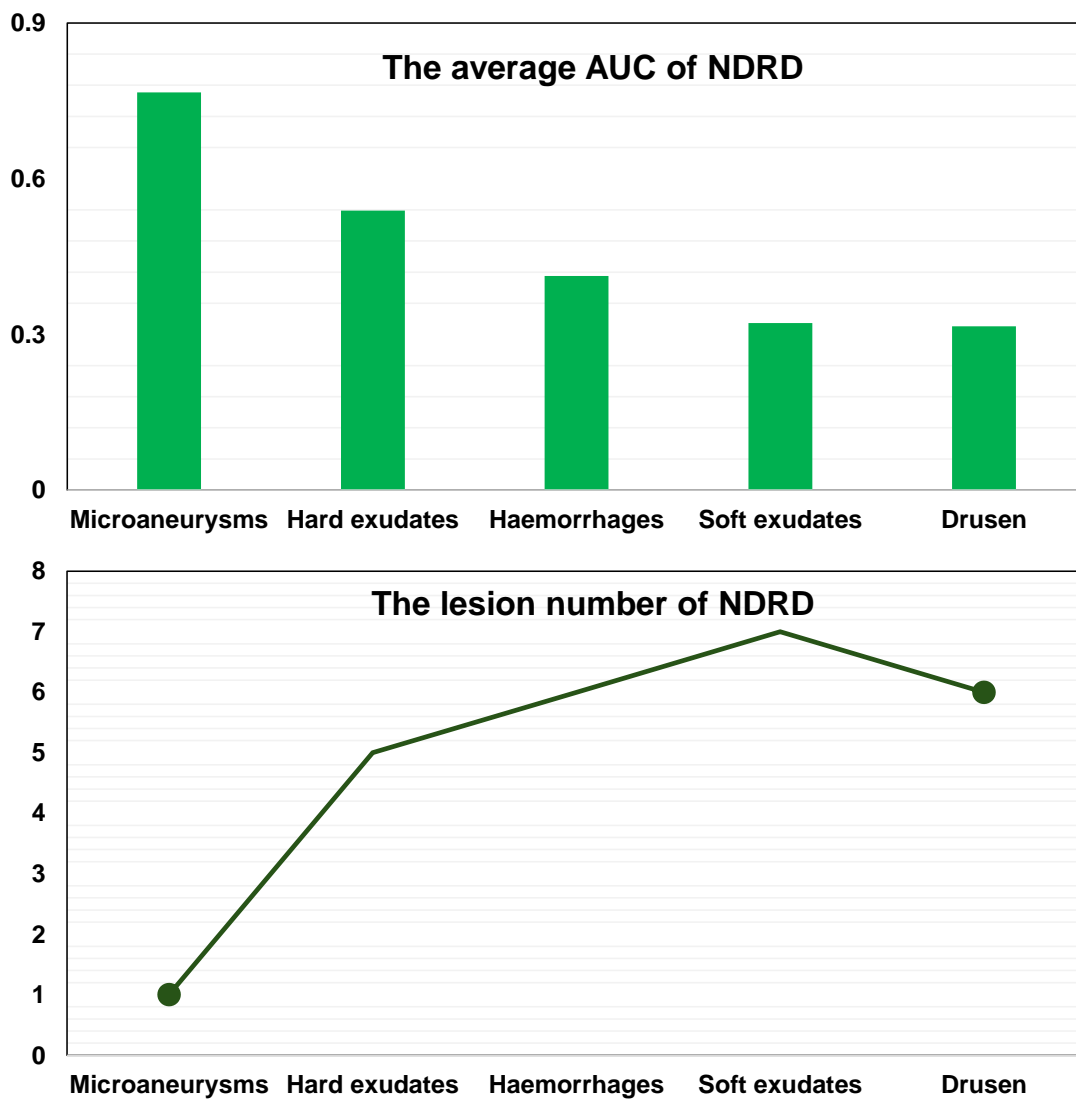
**Supplementary Figure 3. Visual comparison of the binary lesion segmentation results.** Of note, different colors in the original annotated lesion segmentation maps represent different lesions. Besides, the baseline model denotes the referenced U-shape model with the number of fusion layers of one.



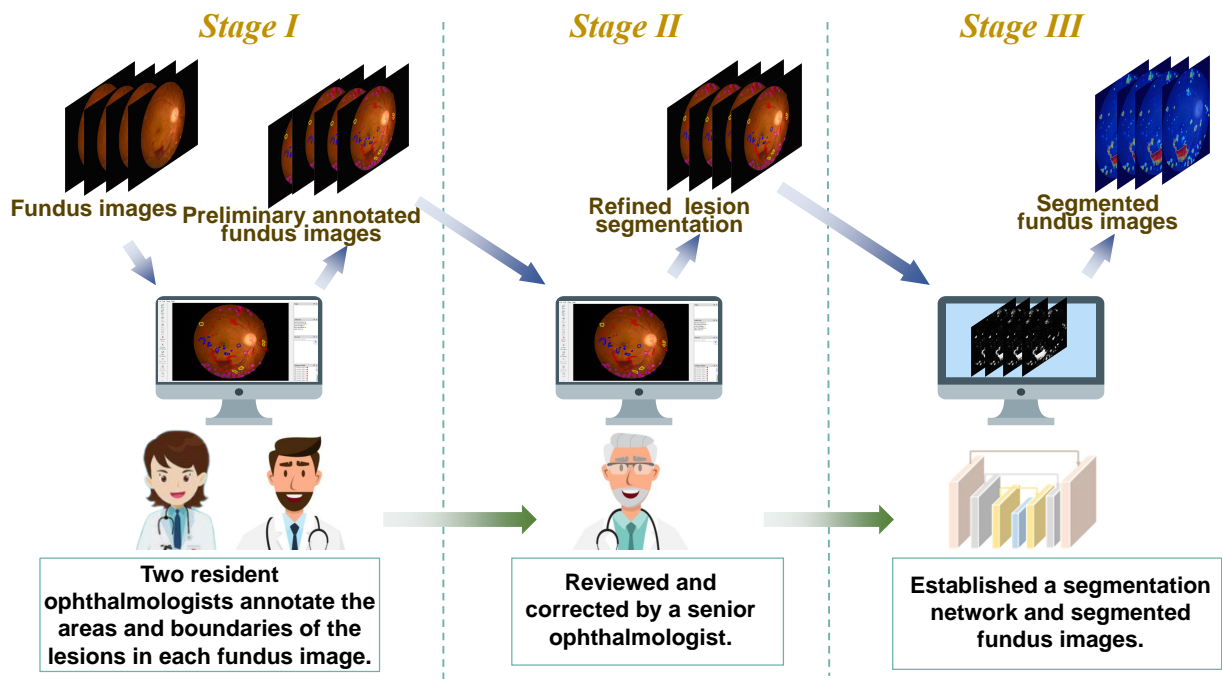
**Supplementary Figure 4. Illustration of the segmented lesion map and network visualization map of DN and NDRD.** A quantitative study of lesion attribution was also performed based on a widely used feature visualization method. Specifically, for each patient diagnosed by the system, we provided both the heatmaps and lesion segmentation of fundus images.

Nephrologists without the AI-assistance			Nephrologists with the AI-assistance			Nephrologists with the visualization maps assistance alone					
A: Nephrologist 1	True			A: Nephrologist 1	True			A: Nephrologist 1	True		
	Prediction	NDRD	DN		Prediction	NDRD	DN		Prediction	NDRD	DN
	NDRD	14	1		NDRD	24	3		NDRD	24	3
DN	10	19	DN	0	17	DN	0	17			
B: Nephrologist 2	True			B: Nephrologist 2	True			B: Nephrologist 2	True		
	Prediction	NDRD	DN		Prediction	NDRD	DN		Prediction	NDRD	DN
	NDRD	13	1		NDRD	21	3		NDRD	21	2
DN	11	19	DN	3	17	DN	3	18			
C: Nephrologist 3	True			C: Nephrologist 3	True			C: Nephrologist 3	True		
	Prediction	NDRD	DN		Prediction	NDRD	DN		Prediction	NDRD	DN
	NDRD	16	8		NDRD	23	2		NDRD	23	3
DN	8	12	DN	1	18	DN	1	17			

**Supplementary Figure 5. The confusion matrix of nephrologists in diagnosing DN and NDRD with or without the AI-assistance.** Three nephrologists further conducted DN and NDRD classification with the summarized principle based on fundus images, network visualization maps and segmented lesion maps.

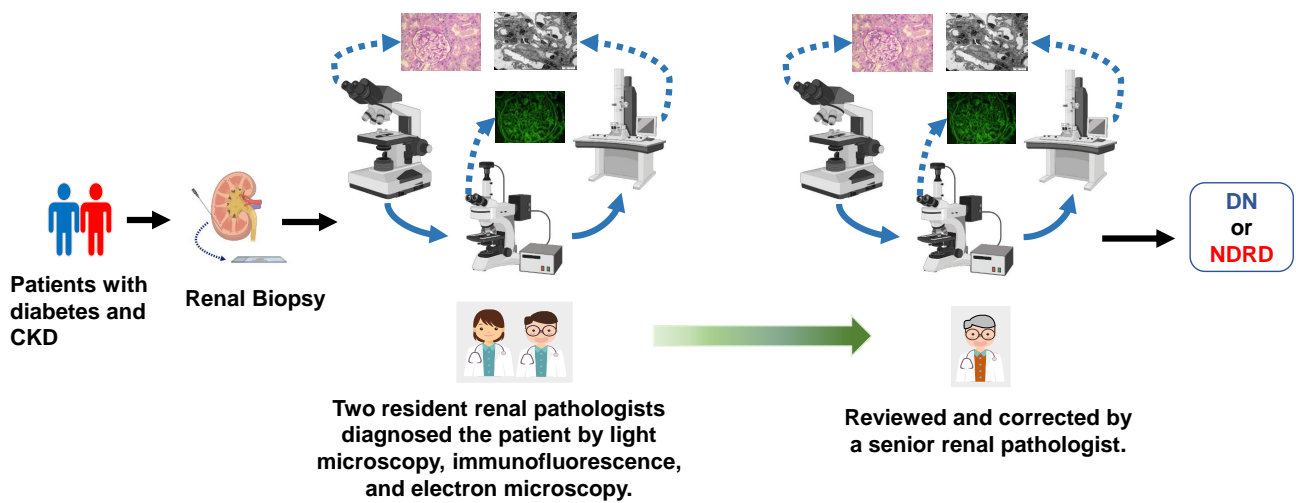


Supplementary Figure 6. The average AUC and lesion number of NDRD. (Top) Average AUC between network visualization maps and lesion segmentation maps. (Bottom) Average lesion number of NDRD per image.

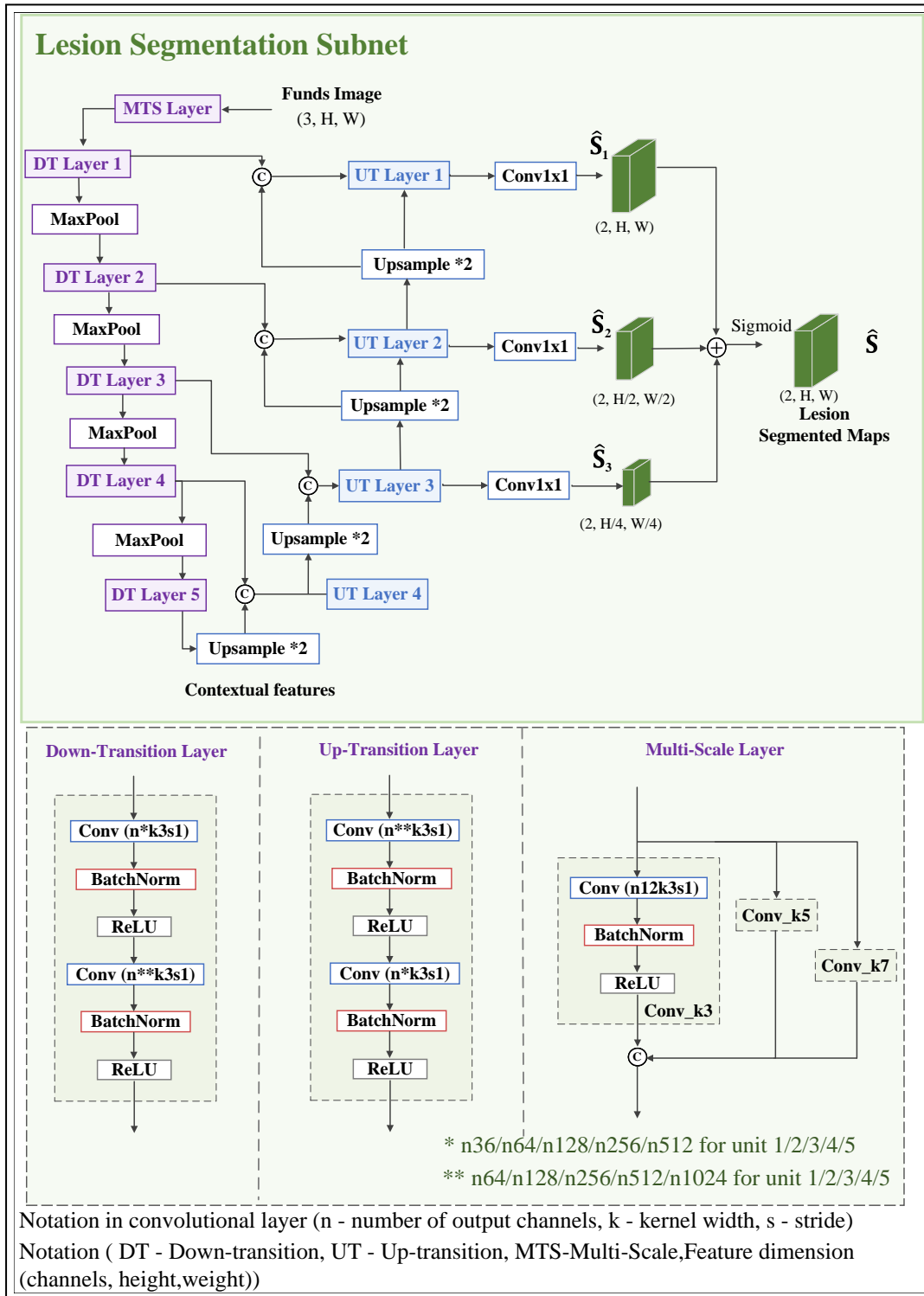


**Supplementary Figure 7. Specific labeling process for fundus lesions.** The fundus lesions were labeled with the LabelMe software by two junior practitioners and reviewed by a senior practitioner with more than 10 years of experience.

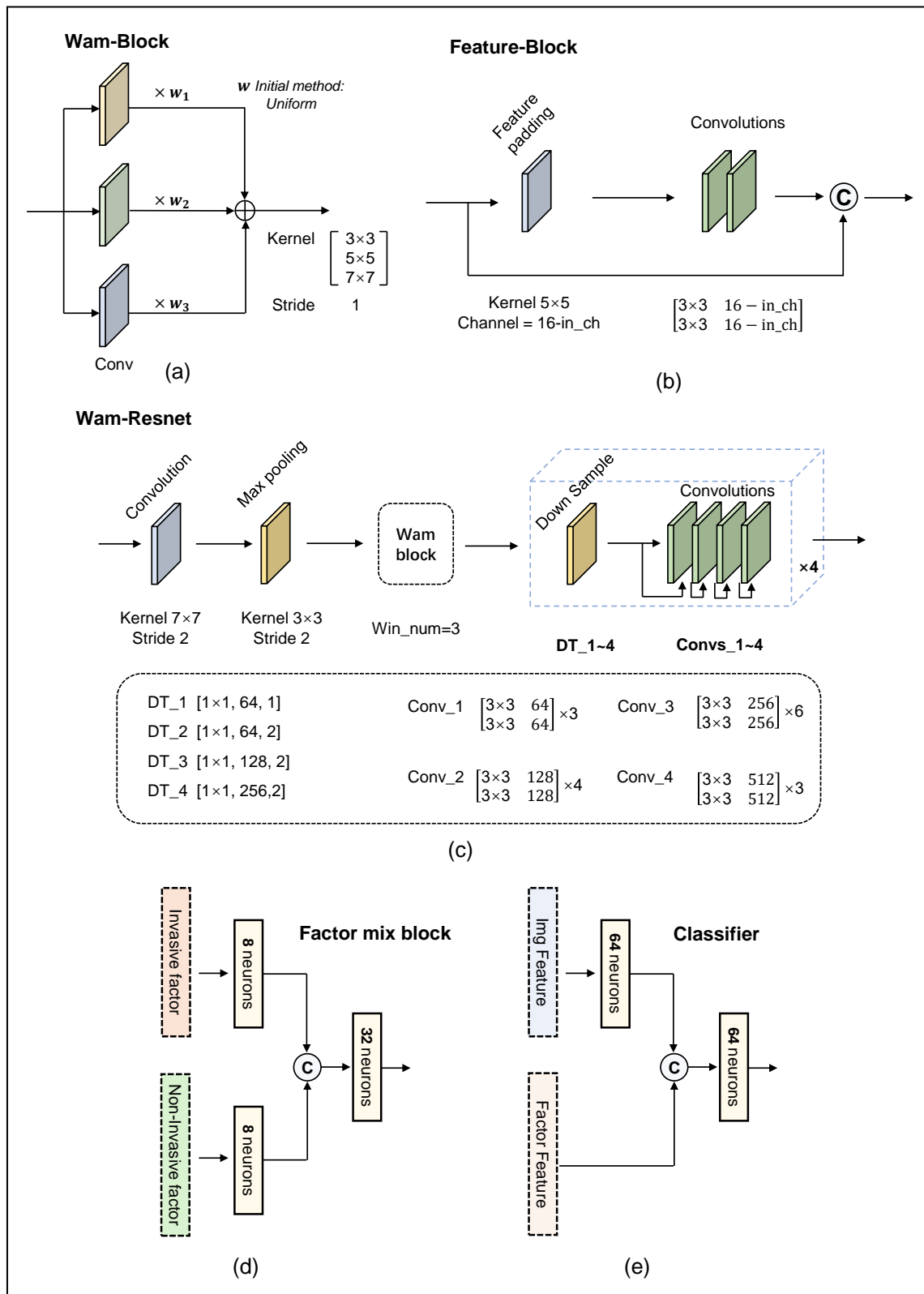




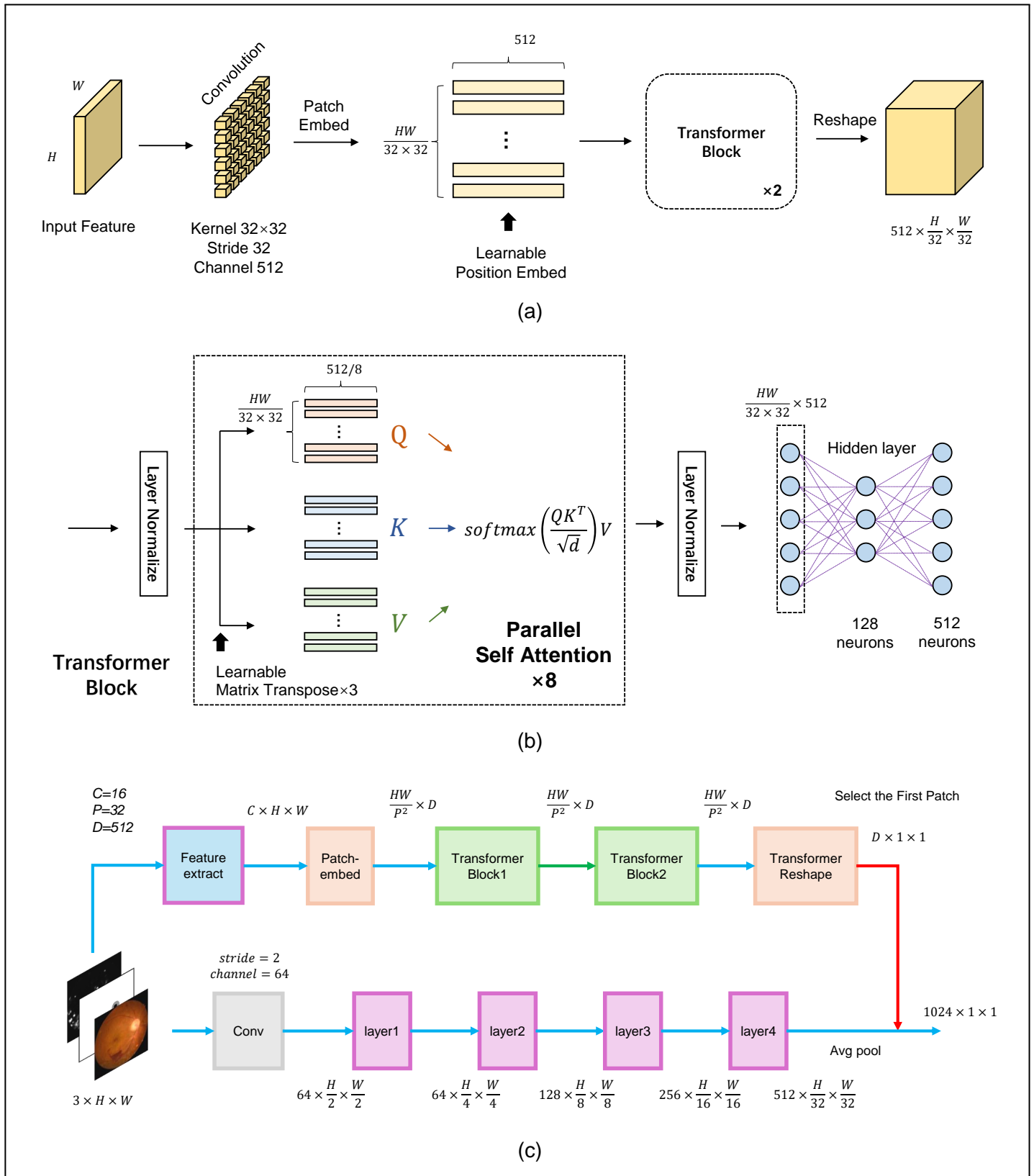
**Supplementary Figure 8. Specific diagnosis process for DN and NDRD.** Kidney biopsy was nonselectively performed in CKD patients with type 2 diabetes. The kidney tissue was examined by light microscopy, immunofluorescence and electron microscopy using standard procedures. Kidney specimens were stained with hematoxylin-eosin, periodic acid–Schiff, hexamine-silver, and immunofluorescence and electron microscopy were used to confirm the diagnosis of DN or NDRD. DN: diabetic nephropathy; and NDRD: nondiabetic renal disease.



**Supplementary Figure 9. Details of the proposed lesion segmentation subnet.** Our lesion segmentation subnet is based on U-shape network, consisting of five down-translation layers and four up-translation layers



**Supplementary Figure 10. The network architecture diagram of CNN part and MLP.** a) the specific structure diagram of windows attention mechanism, which includes three parallel convolutional kernels of different sizes and learnable parameters. b) the specific structure diagram of Feature block. c) the specific structure diagram of Wam-Resnet. The dashed lines enclose four concatenated layers. Note that  $[k \times k, c, s]$  respectively refer to the convolution kernel size, number of channels, and stride size. When  $c$  is set to its default value, the number of channels remains unchanged. The default value for stride is 1. d) the network structure of the Factor Mix Block. e) the network structure of the Classifier.



**Supplementary Figure 11. Description of the structure of the Transformer module.** a) the shape of the feature map changes through the Transformer module. b) Specific computation process of the Transformer block. c) The dimensions and size of the feature maps change in image fusion sub-networks.

**Supplementary Table 1. Pixel-level lesion annotation details of our Retina-DKD set.**

Lesion/Disease	DN (n = 414 images)		NDRD (n = 115 images)	
	Total lesions	Lesions per patient	Total lesions	Lesions per patient
Soft exudates	799	1.93±3.70	229	1.99±2.42
Haemorrhages	5032	12.15±14.90	419	3.64±11.26
Hard exudates	7292	17.61±24.72	389	3.38±7.69
Drusen	601	1.45±16.31	763	6.63±22.92
Neovascularization	29	0.07±0.41	1	0.01±0.09
Microaneurysms	171	0.41±1.13	8	0.07±0.34
Pigmentation	34	0.08±0.88	7	0.06±0.30
retinitis pigmentosa atrophy	1	0.00±0.05	4	0.03±0.18
Preretinal macular membrane	13	0.03±0.20	8	0.07±0.25
Fibre-added membrane	63	0.15±0.67	-	-
Discus opticus membrane	13	0.03±0.19	-	-
Old preretinal hemorrhage	6	0.01±0.17	-	-
Retinal detachment	11	0.03±0.22	-	-
Microvascular proliferation	10	0.02±0.26	-	-
Epiretinal membrane	4	0.01±0.10	-	-
Edama	-	-	2	0.02±0.13
Vitreum floats	-	-	51	0.44±2.46
All lesions	14079	34.01±36.83	1881	16.36±26.15

**Supplementary Table 2. Classification performance of nephrologists with or without AI-assistance.**

The classification performance of nephrologists without AI-assistance.

Nephrologists	Accuracy	Sensitivity	Specificity	Precision	F1 score
Nephrologist 1	75.00%	58.33%	95.00%	93.33%	71.79%
Nephrologist 2	72.70%	54.17%	95.00%	92.86%	68.42%
Nephrologist 3	63.60%	66.67%	60.00%	66.67%	66.67%
Average	70.43%	59.72%	83.33%	84.29%	68.96%

The classification performance of nephrologists with AI-assistance.

Nephrologists	Accuracy	Sensitivity	Specificity	Precision	F1 score
Nephrologist 1	93.20%	100.0%	85.00%	88.89%	94.12%
Nephrologist 2	86.40%	87.50%	85.00%	87.50%	87.50%
Nephrologist 3	93.20%	95.83%	90.00%	92.00%	93.88%
Average	90.93%	94.44%	86.67%	89.46%	91.83%

The classification performance of nephrologists with the visualization maps assistance alone.

Nephrologists	Accuracy	Sensitivity	Specificity	Precision	F1 score
Nephrologist 1	93.20%	100.0%	85.00%	88.89%	94.12%
Nephrologist 2	88.64%	87.50%	90.00%	91.30%	89.36%
Nephrologist 3	90.91%	95.83%	85.00%	88.46%	92.00%
Average	90.92%	94.44%	86.67%	89.55%	91.83%

**Supplementary Table 3. Results of the ablation study on four validation sets.**

Method	Modality	Accuracy (%)	Sensitivity (%)	Specificity (%)	F <sub>1</sub> -score (%)	AUC (%)
<b>Retina-DKD</b>						
Trans-MUF w/o Img.	Factor	89.3 (89.1-89.8)	90.6 (90.5-91.4)	87.5 (86.9-88.1)	90.6 (90.3-91.0)	90.2 (88.6-90.4)
Trans-MUF w/o Seg.	Img+Fac	87.1 (86.9-87.5)	84.9 (84.6-85.4)	90.0 (89.7-90.5)	88.2 (88.0-88.6)	94.0 (93.9-94.4)
Trans-MUF w/o Fac.	Image	91.4 (90.9-91.4)	98.1(98.1-98.4)	82.5 (81.2-82.3)	92.9 (92.4-92.9)	94.3 (93.8-94.3)
Trans-MUF w/o Trans.	Img+Fac	92.5 (92.3-92.8)	90.6 (90.6-91.3)	95.0 (94.4-95.0)	93.2 (93.0-93.5)	96.6 (96.4-96.7)
Trans-MUF w/o CNN.	Img+Fac	91.4 (91.2-91.7)	90.6 (90.3-91.0)	92.5 (92.2-93.0)	92.3 (92.1-92.5)	96.8 (96.6-96.9)
Vgg with Fac.	Img+Fac	91.4 (91.3-91.8)	86.7 (86.8-87.6)	97.5 (97.1-97.5)	92.0 (91.8-92.3)	96.7 (96.5-96.8)
Trans-MUF.	Img+Fac	93.6 (93.2-93.8)	100 (100-100)	85.0 (84.3-85.6)	94.6 (94.2-94.8)	<b>98.0(97.9-98.0)</b>
<b>Prospective validation</b>						
Trans-MUF w/o Img.	Factor	83.8 (83.5-84.4)	86.3 (85.9-86.8)	76.5 (75.6-77.7)	88.9 (88.5-89.2)	95.2 (93.9-95.0)
Trans-MUF w/o Seg.	Img+Fac	90.4 (90.3-90.8)	88.2 (88.1-88.76)	97.1 (96.8-97.4)	93.3 (93.2-93.5)	96.1 (96.0-96.3)
Trans-MUF w/o Fac.	Image	86.8 (86.4-87.0)	93.1 (92.7-93.2)	67.7 (66.7-68.4)	91.4 (91.0-91.5)	90.6 (90.2-90.8)
Trans-MUF w/o Trans.	Img+Fac	93.4 (93.2-93.6)	95.1 (94.9-95.3)	88.2 (87.7-88.8)	95.6 (95.4-95.7)	98.6 (98.5-98.7)
Trans-MUF w/o CNN.	Img+Fac	90.4 (90.1-90.6)	88.2 (87.8-88.4)	97.1 (96.8-97.4)	93.2 (93.0-93.4)	98.9 (98.8-98.9)
Vgg with Fac.	Img+Fac	90.4 (90.2-90.7)	90.2 (89.8-90.5)	91.1 (90.8-91.8)	93.4 (93.2-93.5)	97.9 (97.8-98.0)
Trans-MUF.	Img+Fac	96.3 (96.3-96.8)	95.1 (95.1-95.7)	100 (100-100)	97.5 (97.5-97.8)	<b>98.9(98.7-99.0)</b>
<b>Multicenter validation</b>						
Trans-MUF w/o Img.	Factor	67.3 (66.7-67.9)	82.6 (82.2-83.7)	56.3 (55.2-56.7)	67.9 (66.9-68.3)	72.2 (68.9-72.9)
Trans-MUF w/o Seg.	Img+Fac	78.2 (78.1-78.8)	82.6 (82.4-83.4)	75.0 (74.8-75.8)	76.0 (75.6-76.5)	80.4 (80.1-80.9)
Trans-MUF w/o Fac.	Image	81.8 (81.5-82.2)	82.6 (82.0-83.1)	81.3 (80.9-81.8)	79.2 (78.5-79.4)	83.0 (82.6-83.4)
Trans-MUF w/o Trans.	Img+Fac	80.0 (79.8-80.5)	69.6 (69.3-70.5)	87.5 (87.1-87.9)	74.4 (73.9-74.9)	81.8 (81.5-82.4)
Trans-MUF w/o CNN.	Img+Fac	85.5 (85.3-85.9)	78.3 (78.1-79.3)	90.6 (90.2-90.9)	81.8 (81.4-82.2)	91.2 (91.0-91.6)
Vgg with Fac.	Img+Fac	80.0 (79.6-80.3)	69.5 (68.8-70.1)	87.5 (87.0-87.8)	74.4 (73.5-74.5)	83.4 (83.3-84.1)
Trans-MUF.	Img+Fac	85.5 (85.0-85.9)	73.9 (73.2-75.0)	93.8 (93.3-94.1)	81.0 (79.9-81.2)	<b>93.2(93.1-93.9)</b>
<b>Nonstandard validation</b>						
Trans-MUF w/o Img.	Factor	78.6 (78.3-79.3)	64.3 (63.0-65.1)	85.7 (85.7-86.7)	66.7 (65.3-67.0)	87.0 (84.7-88.0)
Trans-MUF w/o Seg.	Img+Fac	78.6 (78.2-78.9)	64.3 (63.0-65.1)	85.7 (85.5-86.3)	66.7 (65.8-67.0)	76.3 (75.4-76.5)
Trans-MUF w/o Fac.	Image	81.0 (80.7-81.7)	85.7 (85.5-87.0)	78.6 (78.0-79.3)	75.0 (74.3-75.7)	82.7 (81.8-85.0)
Trans-MUF w/o Trans.	Img+Fac	85.7 (85.3-85.9)	64.3 (63.3-64.8)	96.4 (96.2-96.6)	75.0 (73.9-75.1)	86.5 (86.0-86.7)
Trans-MUF w/o CNN.	Img+Fac	85.7 (85.3-85.9)	64.3 (63.3-64.8)	96.4 (96.3-96.7)	75.0 (74.0-75.2)	75.0 (74.0-75.3)
Vgg with Fac.	Img+Fac	85.7 (85.3-85.9)	57.1 (56.2-57.7)	100.0 (100.0-100.0)	72.7 (71.5-72.8)	85.7 (86.2-86.1)
Trans-MUF.	Img+Fac	85.7 (85.2-86.0)	64.3 (63.1-65.3)	96.4 (96.1-96.7)	75.0 (73.2-75.0)	78.6 (77.8-83.2)

**Supplementary Table 4. P value and 95% confidence interval for each variable screening in univariate logistic regression.** Of note, DM: diabetes duration; eGFR: estimated glomerular filtration rate; ALB, albumin; Hb: hemoglobin; SBP, systolic blood pressure; HbA1c, glycosylated hemoglobin; DBP, diastolic blood pressure; BUA, blood uric acid; and BMI, body mass index.

<b>Variables</b>	<b>P</b>	<b>HR (95%CI)</b>
Sex	0.93	0.98(0.56,1.70)
BMI	0.223	0.96(0.89,1.03)
DM	<0.001	1.01(1.01,1.01)
SBP	<0.001	1.03(1.02,1.04)
DBP	0.628	1.01(0.99,1.03)
eGFR	<0.001	0.98(0.97,0.99)
ALB	0.172	1.02(0.99,1.05)
Hb	<0.001	0.98(0.96,0.99)
HbA1c	0.035	1.11(1.00,1.22)
Cholesterol	0.449	0.97(0.88,1.06)
Fibrinogen	0.566	1.05(0.89,1.25)
Triglyceride	0.755	0.99(0.89,1.09)
BUA	0.285	1.00(0.99,1.00)
24-hr proteinuria	0.061	1.09(1.00,1.18)
Hematuria	0.058	1.64(0.98,2.74)